

## Use of 2D image analysis method for measurement of short fibers orientation in polymer composites

Z. Sadik<sup>a</sup>, E. Ablouh<sup>b</sup>, M. Sadik<sup>c</sup>, K. Benmoussa<sup>c</sup>, H. Idrissi-Saba<sup>a</sup>, H. Kaddami<sup>b</sup> and F. Z. Arrakhiz<sup>d\*</sup>

<sup>a</sup>Laboratory of Metrology and Information processing, Ibn Zohr University, Faculty of Sciences, Agadir, Morocco

<sup>b</sup>Laboratory of Organometallic and Macromolecular chemistry-Composites Materials, Cadi Ayyad University, Faculty of Sciences and Technologies, Marrakech, Morocco

<sup>c</sup>Laboratory of Engineering Sciences, Ibn Zohr University, Faculty of Sciences, Agadir, Morocco

<sup>d</sup>Laboratory of electronics, signal processing and physical modelling, Ibn Zohr University, Faculty of Sciences, Agadir, Morocco

### ARTICLE INFO

#### Article history:

Received 18 October 2019

Accepted 8 January 2020

Available online

9 January 2020

#### Keywords:

Composites

Fiber orientation

Orientation tensor

Image processing

### ABSTRACT

The study and determining of fibre-orientation with a two-dimensional (2D) image analysis of cross-sections is a fast and efficient way to get the fibre orientation distribution over a wide specimen area. There are several techniques for measuring fiber-orientation; however, the present study is based on a technique for the sake of obtaining better results. In this work, we utilize second moments technique to determine fibre orientation state by the use of a Scanning Electron Microscope (SEM) images. In order to determine the fiber-orientation state, a second order orientation tensor is employed. A thermoplastic matrix containing 5, 10, 15, 20, 25 and 30% by weight of hemp fiber is molded using an injection molding machine to obtain dumbbell samples. The orientation tensor is determined by employing geometric parameters of fibers on cross-sections. The geometric parameters are calculated by using image analysis, which employs a computational code especially developed to obtain a tensor components.

© 2020 Growing Science Ltd. All rights reserved.

## 1. Introduction

In recent years, the use of the composite materials has greatly increased in the industrial field. This is due to the performance particularly in the automotive industry (Mortazavian & Fatemi, 2015). The physical properties of fibrous composites are dependent on the types and the quality of their reinforcement according to Maya et al. (2017). In particular, natural short fiber reinforced composites represent a broad category of technical and industrial application, because of their low density, biodegradability, ability to absorb sound waves and the facility of recycling and economical interest as seen by Czigany (2004). The inclusion of these fibers in the polymer matrix considerably reduces its thermal expansion according to Kaczmar et al. (2007). The performance of these materials depends particularly on its microstructure. In addition, the microstructure of composite depends on the manufacturing process and the characteristics of the short fiber such as the ratio, length, and orientation.

\* Corresponding author.

E-mail addresses: [farrakhiz@uiz.ac.ma](mailto:farrakhiz@uiz.ac.ma) (F. E. Arrakhiz)

© 2020 Growing Science Ltd. All rights reserved.

doi: 10.5267/j.esm.2020.1.001

The majority of short fibers reinforced thermoplastics are fabricated using injection or compression molding processes. During the molding process, the fibers are oriented depending on the parameters of the process which influence the flow of the polymer and the fibers, and this highly impacts the physical properties as demonstrated by Ko and Youn (1995) and Lee et al. (1997, 2002). This means that the mechanical properties are strongly dependent on the fibers orientation in the composite. In these processes, very often, the fiber orientation states are predicted by numerical simulations. Real structural characterization is important to validate these numerical predictions. However these characterizations methods are fraught with difficulties.

In fact, several methods have been established to analyse fiber orientation in the composite. The most widely used ways were based on the digital image processing technique. For instance, the Hough transform and the template method have been used for measuring the fiber orientation as shown by Yang and Colton (1994), but these methods are valid only if the fibers are aligned in the 3-axis directions. Furthermore, the determination of the short fiber orientation in a random state is difficult according to Yong et al. (2008). O'Connell and Duckett (1991) used image analyzer COSMOS to measure fiber orientation, whereas Bay and Tucker III (1992) introduced the second order orientation tensor to determine the short fiber orientation state. The latter method is based on the geometry of the fiber cross-section. As referenced by Mlekusch (1999), the author has used some statistical method based on least squares technique to describe the elliptical parameters of fiber cross-section. In fact, Stobie (1986) concludes that the second moment technique is the most useful technique to determine the shape and orientation of fibers, because this method is clear and more simple at the computation level.

In this work, we have used the second moments technique for determining the orientation of the short fibers, the elliptical parameters and hence fiber orientation from fiber cross sections. In fact, the composites samples obtained by injection molding processing technique were cut in the form of cross sections covering a sufficient area which contains a large number of fiber. The surfaces were polished to obtain a good quality SEM images, in which each fiber appearing as ellipse is described in polar coordinates by two angles ( $\theta, \varphi$ ) relative to the cutting plane. To define fiber orientation, we need to calculate the second-order orientation tensor which can be possible by 2D image analysis of fibers from polished cross-sections.

## 2. Theory

### 2.1 Mathematical description of fiber orientation

The orientation of individual fiber can be represented by the components of a unit vector  $p$  which is defined by two angles  $\theta$  and  $\varphi$ ; the  $\theta$  angle is formed by both the fiber direction and axis (ox), but  $\varphi$  is an angle formed by the fiber projection on (oy) and (oz) as illustrated in Fig. 1.

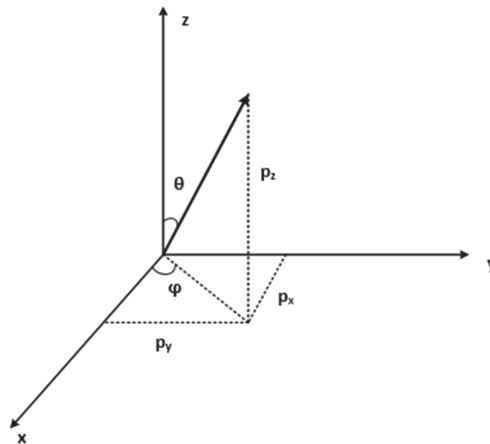


**Fig. 1.** Orientation of a single fiber in polar coordinates.

The components of  $p$  are related to  $\theta$  and  $\varphi$  as follows,

$$\begin{cases} p_x = \sin(\theta) \sin(\varphi) \\ p_y = \sin(\theta) \cos(\varphi) \\ p_z = \cos(\theta) \end{cases} \quad (1)$$

## 2.2 Orientation functions

The fiber orientation distribution function  $\psi(p)=\psi(\theta,\varphi)$  can be defined theoretically as the probability to find a fiber between the angles  $\theta_1$  and  $(\theta_1+d\theta_1)$  and between  $\varphi_1$  and  $(\varphi_1+d\varphi_1)$ ; this probability can be expressed as follows (Tucker III, 1991):

$$P(\theta_1 \leq \theta \leq \theta_1 + d\theta, \varphi_1 \leq \varphi \leq \varphi_1 + d\varphi_1) = \psi(\theta_1, \varphi_1) \sin(\theta_1) d\theta d\varphi. \quad (2)$$

Since two fibers at angles  $(\theta,\varphi)$  and  $(\pi-\theta,\varphi+\pi)$  are not distinguishable, the distribution function has the following symmetry conditions (Tucker III, 1991):

$$\psi(p) = \psi(-p) \quad \theta \rightarrow \pi - \theta, \quad \varphi \rightarrow \varphi + \pi, \quad (3)$$

which means that  $\Psi(p)$  is an even function. In addition,, this function is subject to the following normalization condition (Tucker III, 1991):

$$\int_{-\frac{\pi}{2}}^{\frac{\pi}{2}} \int_0^{\pi} \psi(\theta, \varphi) \sin(\theta) d\theta d\varphi = \int_{\Omega} \psi(p) dp = 1 \quad (4)$$

## 2.3 Tensor description of fiber orientation

The distribution function is not practical to calculate numerically the orientation but precisely describes the orientation fiber state by using the second-and fourth-order orientation tensors. The components of orientation tensors are defined respectively as follows (Advani et al., 1987):

$$a_{ij} = \int_{\Omega} p_i p_j \psi(\vec{p}) d\vec{p} = \langle p_i p_j \rangle \quad (5)$$

$$a_{ijkl} = \int_{\Omega} p_i p_j p_k p_l \psi(\vec{p}) d\vec{p} = \langle p_i p_j p_k p_l \rangle \quad (6)$$

If we consider the second-order tensor, it has nine components, but only six of them are independent because of the symmetry condition. The components of this tensor for a group of  $n$  fibers are calculated as follows (Advani, et al., 1987) :

$$a_{ij} = \frac{1}{n} \left( \sum_{k=1}^n p_i^k p_j^k \right) = \begin{pmatrix} a_{11} & a_{12} & a_{13} \\ a_{21} & a_{22} & a_{23} \\ a_{31} & a_{32} & a_{33} \end{pmatrix} i, j = 1, 2, 3. \quad (7)$$

The components of orientation tensors for an individual fiber  $k$ , are described as follows :

$$\begin{cases} a_{11}^k = \sin^2 \theta^k \cos^2 \varphi^k \\ a_{22}^k = \cos^2 \theta^k \cos^2 \varphi^k \\ a_{33}^k = \cos^2 \theta^k \end{cases} \quad (8)$$

$$\begin{cases} a_{12}^k = a_{21}^k = \sin^2\theta^k \cos\varphi^k \sin\varphi^k \\ a_{13}^k = a_{31}^k = \sin\theta^k \cos\theta^k \cos\varphi^k \\ a_{23}^k = a_{32}^k = \sin\theta^k \cos\theta^k \sin\varphi^k \end{cases} \quad (9)$$

According to the transformation rules of tensors, the latter is symmetric  $a_{ij}=a_{ji}$ , and the normalization condition is given by  $(a_{11}=a_{22}=a_{33}=1)$  (Advani, et al., 1987).

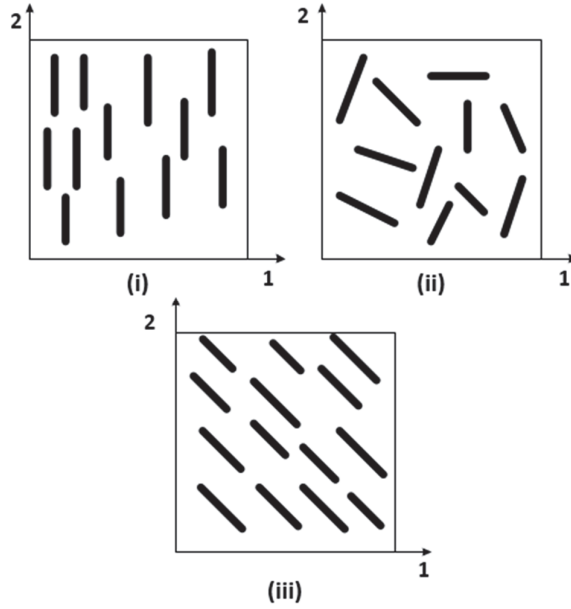


**Fig. 2.** Three examples of orientation distributions of fibers.

The different orientation states of fibers and their orientation tensors are represented in Fig.2. When the fibers are aligned to the principal axes  $x$ ,  $y$ , and  $z$ , as shown in Fig. 2 (i), all the fibres are taking one direction; while fibres are randomly oriented as shown in Fig. 2 (ii), then the orientation tensor is diagonalised. The non-zero values off-diagonal components imply that fibers are not aligned to the  $x$ ,  $y$  and  $z$  direction as shown in Fig.2 (iii). The probability to cut a fiber randomly distributed in a cutting plane, is written as follows (Zhu, et al., 1997).

$$p(\theta) = L\cos\theta + D\sin\theta, \quad (10)$$

where  $L$  and  $D$  are respectively length and diameter of fiber, and  $\theta$  is the angle between the fiber height and axis perpendicular to the section plane, as shown in Fig. 3.

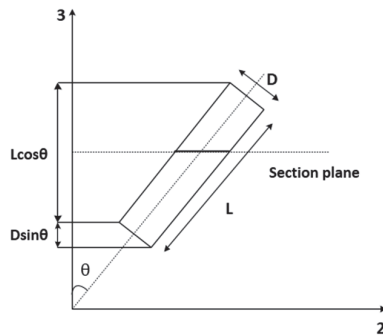


**Fig. 3.** The probability that a fibre of length  $L$  and diameter  $D$  is cut by a section plane proportional to its orientation angle  $\theta$

The correct estimate of orientation tensor is needed for using another approach that is based on the weighting function. This function is represented by the projection of the fiber height on the axis perpendicular to the plane. Therefore, the expression of the orientation tensor becomes (Darlington & Smith, 1987).

$$a_{ij} = \frac{\sum_{k=1}^n F^k a_{ij}^k}{\sum_{k=1}^n F^k} \quad (11)$$

$$F^k = \frac{1}{p(\theta)} = \frac{1}{L\cos\theta + D\sin\theta} \quad (12)$$

where  $F^k$  is called the weighting function.

### 3. 2D Image analysis techniques

#### 3.1 Image analysis

We first start our study by using image analysis: the image is converted to a gray scale image, then we apply the segmentation, thresholding and binarization. To detect the location of the fiber in image, we employ a mathematical programme elaborated with Matlab software. Matlab program is based on two types of descriptors: the first one consists of determining the length of boundary of an irregular object in the binary image, and the second one consists of performing the shape and describing parameters and proprieties of the objects such as moments, area, centroid, moment of inertia and orientation of the object.

The measurement of components of the vector  $p$  for each fiber using 2D image analysis needs certain preparation. First, the specimen in the form of a circular cross-section in planes  $(x, y)$  perpendicular to the flow direction. Secondly, the polishing of a cross-section surface (Mlekuscbgrh, et al., 1997) is needed. The fibers appear as ellipses on the cutting plane.

Different techniques have been developed to measure elliptical parameters. Using binary image analysis, we can find Hough transform by least squares (Yang & Colton, 1994), the geometry of the fiber cross-section and second moments technique (Bay et al., 1992). The second moments technique is still clear and a simple method to determine the short fiber orientation state using the second order orientation tensor.

#### 3.2 Second moments technique

The principle of this technique is used to describe the properties of an object such as position and orientation parameters. First, through a simple threshold, the image is converted into a binary one. Objects can be fetched in the image through pixel connectivity, where sets of pixels are sufficiently large to the extent that all the pixels within the object are added to the set. The second moments are determined during the formation of object (connecting pixels) (Stobie, 1986). They are related to the ellipse parameters by these relations with  $M$  and  $m$  the major and minor axis length of elliptical cross-section fiber (Eberhardt et al., 2001):

$$\begin{cases} M^2 = 2(I_{xx} + I_{yy}) + 2\sqrt{(I_{xx} + I_{yy})^2 + 4I_{xy}^2}, \\ m^2 = 2(I_{xx} + I_{yy}) - 2\sqrt{(I_{xx} + I_{yy})^2 + 4I_{xy}^2}, \end{cases} \quad (13)$$

$$\begin{cases} \varphi = \frac{1}{2} \arctan\left(\frac{2I_{xy}}{I_{yy} - I_{xx}}\right) \\ \theta = \frac{1}{2} \arccos\left(\frac{M}{m}\right) \end{cases} \quad (14)$$

where  $I_{xx}$ ,  $I_{yy}$  and  $I_{xy}$  are the object's second moments of inertia.

## 4. Experimental details

### 4.1 Materials

In this work, we analyzed samples of short hemp fibers which reinforced Polypropylene (PP) matrix. PP matrix is provided by ExxonMobil chemical (density of  $0.9 \text{ g/cm}^3$ , and melting temperature of  $165 \text{ }^\circ\text{C}$ ). NaOH (sodium hydroxide) from, Sigma Aldrich, (purity of, 98%) and  $\text{CH}_3\text{COOH}$  (Acetic acid) from, Riedel-de haën, (purity 99–100%) were used for hemp fibers pretreatment (Le Troedec, et al., 2008; Rokbi et al., 2011) for getting a good wettability toward the matrix. Styrene-(ethylene-butene)-styrene three block copolymer grafted with maleic anhydride (SEBS-g-MA) was supplied by Shell (KratonFG-1901X) containing 1.4–2 wt.% MA. This copolymer was used as coupling agent to improve the interfacial adhesion between hemp fibers and PP matrix. The hemp fibers were harvested from the Moroccan Rif. They have an average length of  $1450 \text{ }\mu\text{m}$  and an average diameter of  $210 \text{ }\mu\text{m}$ .

### 4.2 Composite preparation

The polypropylene matrix is mixed with a various amounts of hemp fibers (5, 10, 15, 20, 25,30wt.%) using a Leistritz ZSE-18 Twin screw extruder (LEISTRITZ EXTRUSIONSTECH NIK GMBH, Germany), at 125 rpm screw rotating for the matrix and 40rpm screw rotating for the side stuffer. The extruder barrel of seven compartments (zone) was heated at 200,200,200, 200, 180, 180, 180, and  $180 \text{ }^\circ\text{C}$  from the hopper to the die (Pilu, et al., 1996; O'Connell & Duckett., 1991). The composites were cooled in a water bath and then pelletized into granules of 2mm length. The described experimental procedure was used to prepare both composites system.

The final composite samples were molded by using an injection molding machine (Engel e-Victory) (Arrakhiz et al., 2013). The temperature of the injection press barrel was set at  $200 \text{ }^\circ\text{C}$  for the three heating zone. The nozzle temperature was set at  $180 \text{ }^\circ\text{C}$  while the mold was set at  $45 \text{ }^\circ\text{C}$ .

### 4.3 Sample Preparation

The specimens studied in this work were cut from an injected dumbbells with various fiber content, the geometry and dimensions of this dumbbell are shown in Fig. 4. Each specimen is cut normal to the flow direction at four different positions, (position 1~4) as shown in Fig. 4, and each sample was polished by using the metallographic method.

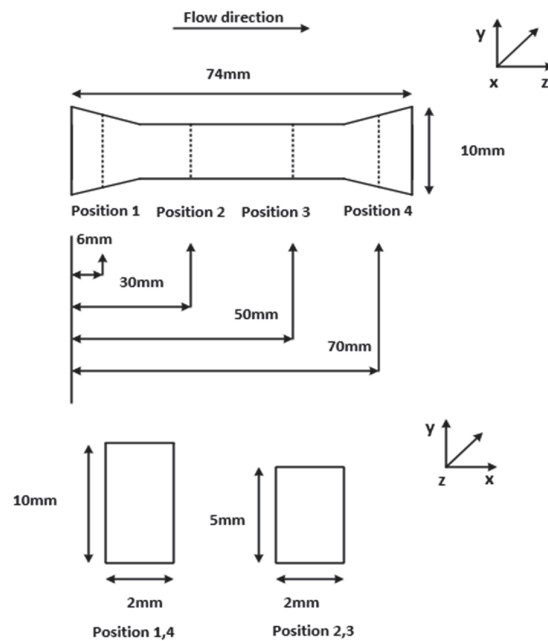


**Fig. 4.** Dimensions of the sample and observed positions.

## 4.4 Characterization

### 4.4.1, Scanning electron microscopy

Scanning electron microscopy (SEM) used to assess the dispersion of fibers in the polymer matrix and to show the morphology of hemp fibers. It was also used to prepare images for thresholding and image treatment (session 4.5). The SEM studies were carried out using a TESCAN VEGA 3 microscope (Acceleration voltage: 10 KV, Working distance :~10 mm). As the materials observed were insulating. The surfaces were treated with an ultrathin layer of carbon by sputtering with a Scancoat Six sputtering machine from Edwards.

### 4.4.2, MATLAB

MATLAB is used to calculate the orientation tensor by using a developed computational code.

### 4.5 Imaging conditions

The images of the polished cross-sections in planes (y, z) perpendicular to the flow direction are realized by using the Scanning Electron Microscope (SEM) as illustrated in Fig. 5(a). Fig. 5(b) shows a cross-section after the transformation of the image (Fig. 5 (a)) into binary images by using the thresholding method.

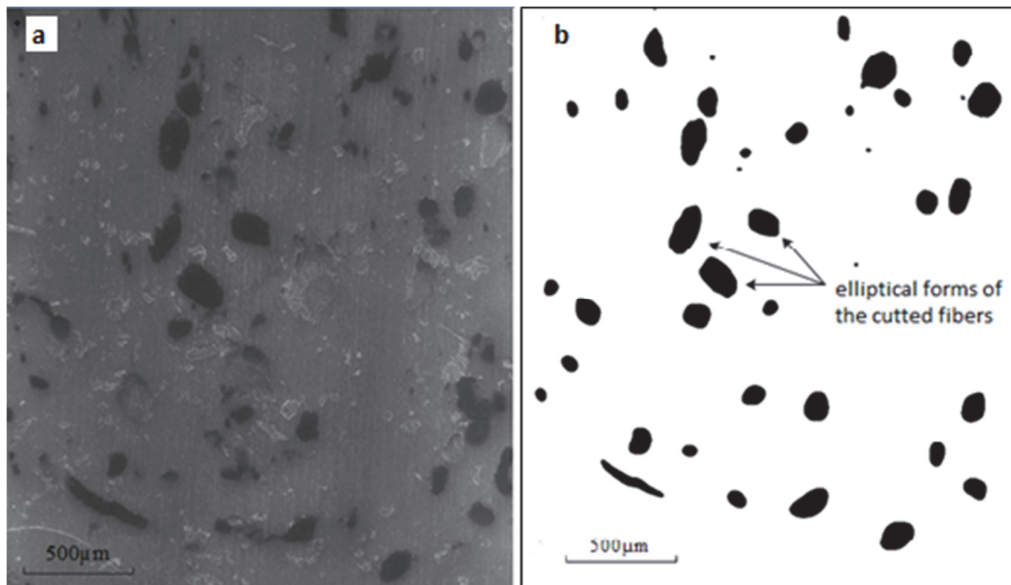


**Fig. 5. (a)** SEM image of sectioning plane of PP/10 wt.% hemp fibers.(b)Typical images after thresholding

The overlapping fiber images which were outside the boundary of the domain were eliminated. Based on these images, we can calculate the fiber orientation states. A computer program is developed to determine the second order orientation tensor from elliptical parameters of the fiber cross-section.

### 4.6 Validation of the program on reference images

Before analysing samples of unknown orientations we need to validate our code. We use a series of known orientation reference images. We chose the very simple case of perfectly unidirectional composites. The results obtained by the matlab analysis are compared with the theoretical results as shown in Fig. 6.

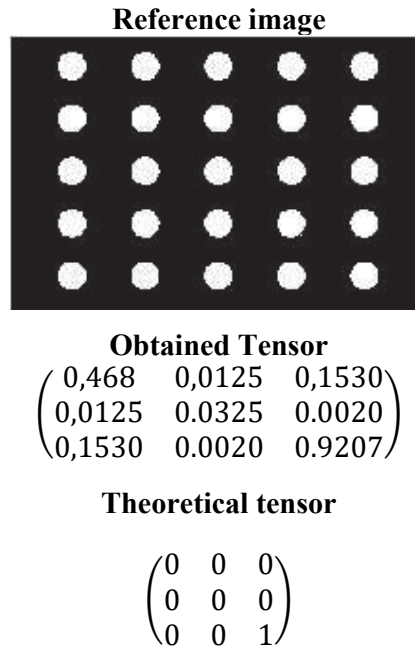


**Fig. 6.** Reference image analysis for unidirectional orientation.

## 5. Results and Discussion

### 5.1 Morphological properties

Fig. 7 shows the fractured surface of the PP based composites filled with 20 wt% of hemp fibers. Different magnifications have been used to assess the fibers dispersion, the hemp fibers structure and the interfacial adhesion. It can be seen that ,the use of a coupling agent decreases the fiber/fiber contact, which allows a good dispersion and distribution into the polymer matrix (Fig.7a and 7b). Moreover, the addition of a coupling agent improves the wettability between the natural fibers and the polymer leading to better adhesion between fibers and the matrix, and reduces pull out fibers, which is found in the composites without coupling agent (Fig. 7c and 7d). On the other hand, these analyses enable to characterize the morphology of hemp fibers. It can be seen that they have a tubular shape with an ellipsoidal section. The magnification of a single fibre reveals that it is constituted of microfibrils (Fig.7 (d)). These analyses also show that the external surface of hemp fibers appears clean, this is due to the alkali treatment that removes impurities from their surface contact, which may also help to improve fiber/matrix surface adhesion (Ku et al., 2011).

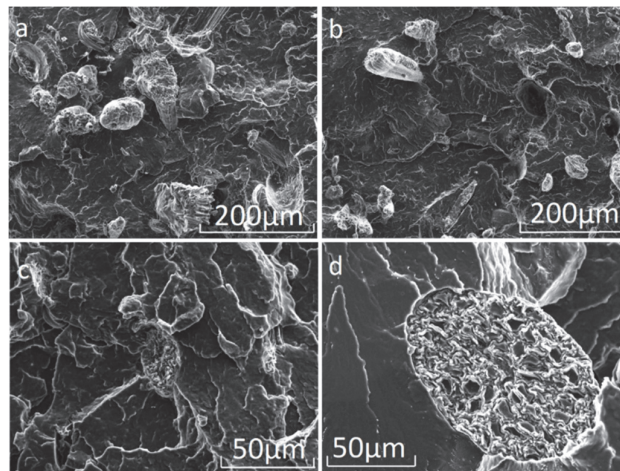


**Fig. 7.** Morphology images of PP-SEBS- g-MA/30 wt.% hemp fibers (Alk).



## 5.2 Orientation States along the Flow Direction

The fiber orientation tensors are accurately determined by analyzing the images obtained with a scanning electron microscope at different positions of the specimen. For example, Figure 8 shows the results of orientation for the composite with wt% of fibers.

We can show in Fig. 8 the diagonal components, which describe the orientation of fibers in the axes  $x$ ,  $y$  and  $z$ . Moreover, the non-zero off-diagonal components mean that the axes  $x$ ,  $y$  and  $z$  are not the principal ones (Tucker & Dessenberger, 1994).

The experimental values of orientation tensor are represented in Fig. 8 (a). We can observe that the values of  $a_{yy}$  and  $a_{zz}$  have high values compared to that of  $a_{xx}$  at position 1-2. That is, the fibers are distributed mainly in the  $y$ - $z$  plane; therefore, the fibers are randomly distributed in this plane. Moreover, the components values  $a_{xx}$ ,  $a_{yy}$  and  $a_{zz}$  at position 3-4 mean that the distribution of fibers are oriented in three dimensions, but they are not strictly random because the value of  $a_{zz}$  is greater than those of  $a_{xx}$  and  $a_{yy}$ . This indicates that the most fibers are parallel to the flow direction.

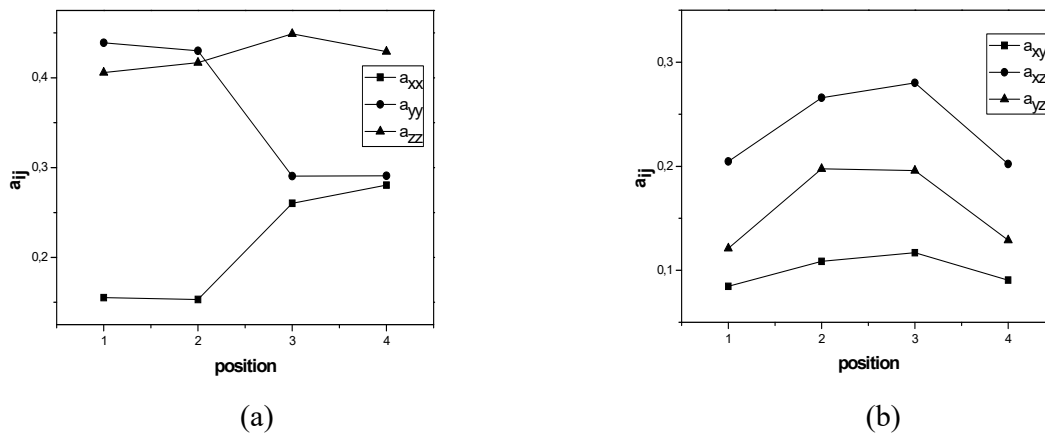


**Fig. 8.** Components of the orientation tensor at different positions: (a) diagonal components, (b) off-diagonal components

On the one hand, off-diagonal components are shown in Fig. 8 (b). It can be observed that  $a_{xy}$  has small values compared to those of  $a_{xz}$  and  $a_{yz}$ . That is, the principal direction of orientation is located in the two planes  $x$ - $z$  and  $y$ - $z$ , and many fibers are partially oriented in the  $x$ - $y$  plane. The components  $a_{zz}$ ,  $a_{xz}$ , and  $a_{yz}$  have high values along this specimen; as a result, most fibers are oriented toward the flow direction. On the other hand, this small difference between the values of components at each position of orientation tensor can be explained by the geometry and dimensions of the specimen. This result shows that a variation of positions along the specimen has no significant influence on the distribution of the final orientation.

## 5.3 Orientation States at different fraction of fibers

We are interested here in samples with 5, 10, 15, 20, 25 and 30 wt. % of hemp fiber. Fig. 9 represents the evolution of orientation tensor at different percentages. In Figure 9, diagonal components are shown in (a) and off-diagonal components in (b). It can be seen that the component  $a_{xx}$  has a large value compared to those of  $a_{yy}$  and  $a_{zz}$  at 5%; this indicates, on the one hand, that a large portion of these fibers are strongly orientated in  $x$ -direction, so they are perpendicular to the flow direction.

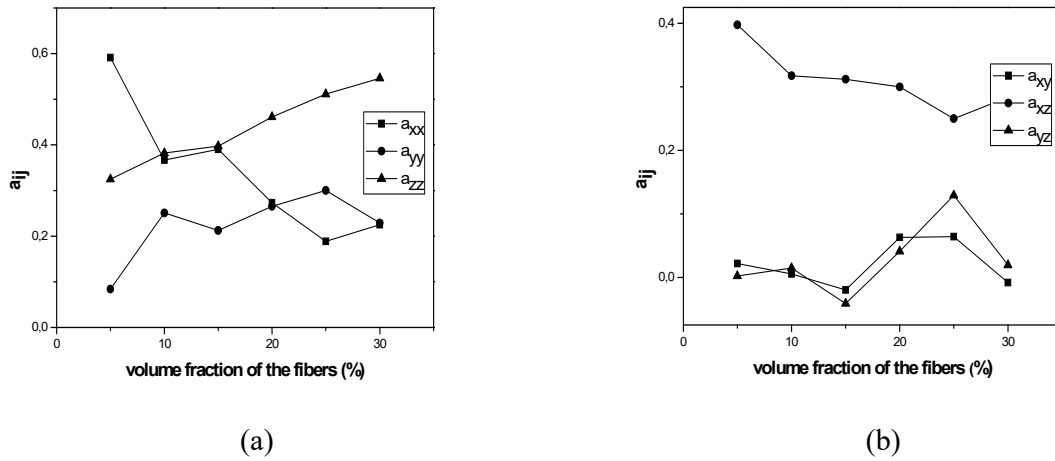


**Fig. 9.** Components of the orientation tensor at different fraction of fibers: (a) diagonal components, (b) off-diagonal components

On the other hand, a small portion of these fibers are aligned in flow direction. The fibers at percentages 10% and 15% are randomly distributed in three directions: x, y and z. As for 20 wt.%, 25 wt.% and 30 wt.%, it can be observed that the values of  $a_{zz}$  are ranging from 0.46 to 0.55, that is to say that, these fibers are largely influenced by the flow in the z direction. Moreover, off-diagonal components  $a_{xy}$  and  $a_{yz}$  have small values compared to that of  $a_{xz}$ , so the distribution of fibers is located in the x-z plane and is outside the two planes x-y and y-z; this explains that many fibers are randomly oriented in the x-z plane. The values of  $a_{xy}$  and  $a_{xz}$  which change their sign from positive to negative. This might imply that these fibers rotate in the opposite side of the two following planes: x-y and y-z. It can be inferred from the results obtained in Fig. 9 (b) that the value of the component  $a_{zz}$  increases with the increasing in fiber percentage.

## 6. Conclusions

The use of the image analysis technique to determine the fiber orientation states is a very fast and efficient method for determining the second order orientation tensor. In this paper, we use the second moments technique for measuring the elliptical parameters of the fibers from their cross sections. A simple computer program is developed to calculate the orientation tensor from geometrical parameters of the fiber cross-section. The orientation tensors are measured at different positions throughout the flow direction and at different fractions of fibers. The results obtained show that the variation in position has no influence on the final fibers orientation, and they are unchanged alongside with the flow path. Moreover, the diagonal components of the orientation tensor indicate that the fibers are randomly oriented in the specimen at a low percentage of fibers, but fibers at a high percentage are strongly oriented in the flow direction.

## Acknowledgement

The authors would like to thank the anonymous referees for constructive comments on earlier versions of this paper.

## References

- Advani, S. G., & Tucker III, C. L. (1987). The use of tensors to describe and predict fiber orientation in short fiber composites. *Journal of Rheology*, 31(8), 751-784.
- Arrakhiz, F. Z., Malha, M., Bouhfid, R., Benmoussa, K., & Qaiss, A. (2013). Tensile, flexural and torsional properties of chemically treated alfa, coir and bagasse reinforced polypropylene. *Composites Part B: Engineering*, 47, 35-41.

- Bay, R. S., & Tucker III, C. L. (1992). Stereological measurement and error estimates for three-dimensional fiber orientation. *Polymer Engineering & Science*, 32(4), 240-253.
- Czigany, T. (2004). An acoustic emission study of flax fiber-reinforced polypropylene composites. *Journal of composite materials*, 38(9), 769-778.
- Darlington, M. W., & Smith, A. C. (1987). Some features of the injection molding of short fiber reinforced thermoplastics in center sprue-gated cavities. *Polymer Composites*, 8(1), 16-21.
- Eberhardt, C., Clarke, A., Vincent, M., Giroud, T., & Flouret, S. (2001). Fibre-orientation measurements in short-glass-fibre composites—II: A quantitative error estimate of the 2d image analysis technique. *Composites Science and Technology*, 61(13), 1961-1974.
- Kaczmar, J. W., Pach, J., & Kozłowski, R. (2007). Use of natural fibres as fillers for polymer composites. *International Polymer Science and Technology*, 34(6), 45-50.
- Ko, J., & Youn, J. R. (1995). Prediction of fiber orientation in the thickness plane during flow molding of short fiber composites. *Polymer composites*, 16(2), 114-124.
- Ku, H., Wang, H., Pattarachaiyakoop, N., & Trada, M. (2011). A review on the tensile properties of natural fiber reinforced polymer composites. *Composites Part B: Engineering*, 42(4), 856-873.
- Le Troedec, M., Sedan, D., Peyratout, C., Bonnet, J. P., Smith, A., Guinebretiere, R., ... & Krausz, P. (2008). Influence of various chemical treatments on the composition and structure of hemp fibres. *Composites Part A: Applied Science and Manufacturing*, 39(3), 514-522.
- Lee, S. C., Yang, D. Y., Ko, J., & Youn, J. R. (1997). Effect of compressibility on flow field and fiber orientation during the filling stage of injection molding. *Journal of Materials Processing Technology*, 70(1-3), 83-92.
- Lee, Y., Lee, S., Youn, J., Chung, K., & Kang, T. (2002). Characterization of fiber orientation in short fiber reinforced composites with an image processing technique. *Materials Research Innovations*, 6(2), 65-72.
- Maya, M. G., George, S. C., Jose, T., Sreekala, M. S., & Thomas, S. (2017). Mechanical properties of short sisal fibre reinforced phenol formaldehyde eco-friendly composites. *Polymers from Renewable Resources*, 8(1), 27-42.
- Mortazavian, S., & Fatemi, A. (2015). Effects of fiber orientation and anisotropy on tensile strength and elastic modulus of short fiber reinforced polymer composites. *Composites part B: engineering*, 72, 116-129.
- Mlekusch, B. (1999). Fibre orientation in short-fibre-reinforced thermoplastics II. Quantitative measurements by image analysis. *Composites Science and Technology*, 59(4), 547-560.
- Mlekusch, B., Lehner, E. A., & Wolfgang, G. (1999). Fibre orientation in short-fibre-reinforced thermoplastics I. Contrast enhancement for image analysis. *Composites science and technology*, 59(4), 543-545.
- O'Connell, P. A., & Duckett, R. A. (1991). Measurements of fibre orientation in short-fibre-reinforced thermoplastics. *Composites Science and Technology*, 42(4), 329-347.
- Pilu, M., Fitzgibbon, A. W., & Fisher, R. B. (1996, September). Ellipse-specific direct least-square fitting. In *Proceedings of 3rd IEEE International Conference on Image Processing* (Vol. 3, pp. 599-602). IEEE.
- Rokbi, M., Osmani, H., Imad, A., & Benseddiq, N. (2011). Effect of chemical treatment on flexure properties of natural fiber-reinforced polyester composite. *Procedia Engineering*, 10(0), 2092-7.
- Stobie, R. S. (1986). The COSMOS image analyser. *Pattern Recognition Letters*, 4(5), 317-324.
- Tucker III, C. L. (1991). Flow regimes for fiber suspensions in narrow gaps. *Journal of Non-Newtonian Fluid Mechanics*, 39(3), 239-268.
- Tucker, C. L., & Dessenberger, R. B. (1994). Flow and rheology in polymer composites manufacturing. *Flow and Rheology in Polymer Composites Manufacturing*.
- Yang, H., & Colton, J. S. (1994). Quantitative image processing analysis of composite materials. *Polymer composites*, 15(1), 46-54.
- Zhu, Y. T., Blumenthal, W. R., & Lowe, T. C. (1997). Determination of non-symmetric 3-D fiber-orientation distribution and average fiber length in short-fiber composites. *Journal of Composite Materials*, 31(13), 1287-1301.



© 2020 by the authors; licensee Growing Science, Canada. This is an open access article distributed under the terms and conditions of the Creative Commons Attribution (CC-BY) license (<http://creativecommons.org/licenses/by/4.0/>).